

## Parametric lightweight design of a direct-drive wind turbine electrical generator supporting structure for minimising dynamic response

P. Jaen-Sola, E. Oterkus & A. S. McDonald

To cite this article: P. Jaen-Sola, E. Oterkus & A. S. McDonald (2021): Parametric lightweight design of a direct-drive wind turbine electrical generator supporting structure for minimising dynamic response, Ships and Offshore Structures, DOI: [10.1080/17445302.2021.1927356](https://doi.org/10.1080/17445302.2021.1927356)

To link to this article: <https://doi.org/10.1080/17445302.2021.1927356>



© 2021 The Author(s). Published by Informa UK Limited, trading as Taylor & Francis Group



Published online: 21 May 2021.



Submit your article to this journal [↗](#)



Article views: 42



View related articles [↗](#)



View Crossmark data [↗](#)

# Parametric lightweight design of a direct-drive wind turbine electrical generator supporting structure for minimising dynamic response\*

P. Jaen-Sola<sup>a</sup>, E. Oterkus<sup>b</sup> and A. S. McDonald<sup>c</sup>

<sup>a</sup>Mechanical and Materials Engineering Department, School of Engineering and the Built Environment, Edinburgh Napier University, Edinburgh, UK; <sup>b</sup>Naval Architecture, Ocean and Marine Engineering Department, University of Strathclyde, Glasgow, UK; <sup>c</sup>School of Engineering, Institute for Energy Systems, The University of Edinburgh, Edinburgh, UK

## ABSTRACT

Heavy, large and robust supporting structures are needed to keep the airgap clearance of direct-drive multi-MW wind turbine electrical generators open and stable. As rotating pieces of machinery, generators vibrate when their natural frequencies are excited introducing potentially large amplitude oscillations due to the forces acting on them that could cause structural fatigue, noise and, in the worst-case scenario, their sudden collapse. A novel procedure for cost-effective and dynamically efficient structural design of a generator has been developed through a series of different finite element studies for a proposed 3MW machine with a conical rotor structure working under extreme conditions. Following a parametric approach coupled with the use of a topology optimisation tool it was demonstrated that the structural mass and dynamic response of the machine can be minimised, while complying with the deflection requirements.

## ARTICLE HISTORY

Received 27 October 2020  
Accepted 3 May 2021

## KEYWORDS

Offshore direct-drive wind turbine; generator structure; parametric approach; topology optimisation; dynamic design

## 1. Introduction



Wind energy is considered as the most mature renewable energy type and has an outstanding role to play in the battle against global warming. With the offshore renewable energy market gathering most of the attention, turbine technology is being developed very rapidly. Wind resources are greater and steadier in deep waters than onshore. However, the sea environment imposes a series of demanding conditions and challenges that can only be tackled using innovative strategies. Machine's components have to deal with high levels of humidity and salt in the air, as well as with significant changes of temperature and in the dynamic loads induced by waves. Direct-driven wind turbines are low-speed machines (rotational speed typically varies between 8 and 15 rpm depending upon the power rating), which were conceived to reduce the complexity of the turbine drivetrain by removing the gearbox and directly coupling the generator to the wind turbine hub. With this, a complex rotating piece of machinery heavily dependent on the capacity of the oil to lubricate and transfer heat between gears with the highest failure rate (Carroll et al. 2016) among the components forming the drivetrain is eliminated.

The main goal of the structural design of an electrical generator is to maintain the airgap clearance between the rotor and the stator open and stable. For that, a typical deflection limit of 10% of the corresponding airgap length in any direction is imposed since the beginning of the design process. This means that heavy and robust supporting structures are necessary in order to withstand transportation, installation, operation and maintenance loads without exceeding the limit.

Although design configurations are numerous and electrical machines are usually customised for each type of turbine following

the generator design standards such as the IEC 61400-1 International Standard (2008), all electrical machines show an arrangement composed by the active material, formed by the electrical subcomponents such as back iron, copper and magnets and the inactive material, which corresponds to supporting structure. Generators can be categorised into electrically excited and permanent magnet excited. Permanent magnet excitation is preferable when aiming for a lighter and more reliable design. Within this category, one can find three different types of configurations: radial-flux, axial-flux and transverse-flux. Machines are characterised according to the orientation of the magnetic flux as it crosses the airgap. Since radial-flux permanent magnet electrical generators are the most common commercial models (Jaen-Sola 2017) and although axial-flux and transverse-flux generators are of significant interest, this investigation focuses on radial-flux machines.

Typically, research has concentrated on optimising the weight of the active material. However, supporting structure is the part accounting for the highest percentage of mass. Hartkopf et al. (1997) found that at least 2/3 of the total mass of radial-flux generator corresponds to inactive material. Several investigations have tried to minimise the structural mass of radial-flux permanent magnet generators using analytical and numerical methods with the aim of estimating the minimum needed stiffness so that the structure can cope with the loads. With the minimum stiffness, ' $k$ ', defined as the ratio between the force applied on a surface, ' $F$ ', and the deflection generated by the force along the same degree of freedom, ' $\delta$ ', ( $k = F/\delta$ ), it is possible to calculate the minimum mass of the structure in a reliable and quick fashion. Figure 1(a) displays the typical generator rotor structures, which are still under investigation, while Figure 1(b) shows a generator structure made of discs fully integrated into the wind turbine.

**CONTACT** P. Jaen-Sola  p.sola@napier.ac.uk  Mechanical and Materials Engineering Department, School of Engineering and the Built Environment, Edinburgh Napier University, Edinburgh EH10 5DT, UK

\*International Conference on Ships and Offshore Structures, ICSOS 2020k, 1–3 September 2020, Glasgow, UK

© 2021 The Author(s). Published by Informa UK Limited, trading as Taylor & Francis Group

This is an Open Access article distributed under the terms of the Creative Commons Attribution-NonCommercial-NoDerivatives License (<http://creativecommons.org/licenses/by-nc-nd/4.0/>), which permits non-commercial re-use, distribution, and reproduction in any medium, provided the original work is properly cited, and is not altered, transformed, or built upon in any way.

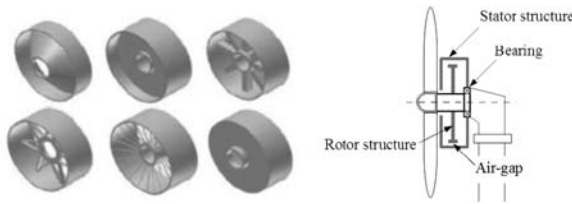


**Figure 1.** (a) Typical rotor structures (Stander et al. 2012); (b) Generator structure (Jaen-Sola 2017).

In (Jaen-Sola 2017), the author made a mass comparison between a spoke-armed structure and a disc structure of a 3MW machine both subjected to the same operational loads revealing a difference of almost of 47% in favour of the disc structure. Since spoked-armed structures do not perform well under torque loads the thickness of the hollow arms needs to be considerably increased with the consequent increase in mass. With a suitable structural configuration identified, Jaen-Sola et al. (2019) carried out an investigation over the suitability of materials with different elastic modulus to density ratios. A comparative study between a 3MW generator structure made of cast iron and another made of carbon epoxy showed the advantages and implications of employing composite materials in the design of these machines (Jaen-Sola et al. 2019). A difference in mass of 60% in favour of the composite structure shed light on the possibilities offered by composite materials when it comes to design a weight sensitive structure.

All of these studies have analysed the structures from a static viewpoint. However, the dynamic behaviour of the machine needs to be carefully considered at the early stages of the design too. A density-based topology optimisation approach was used by Kirschneck (2016) to study potential mass savings of the XD-115 offshore direct-drive wind turbine electrical machine rotor taking its dynamic behaviour into account. A more generic methodology was developed by Jaen-Sola et al. (2018), where a series of contour plots allowing the engineer to accurately estimate the mass and the natural frequencies of the structure were presented. The consequences of implementing distinct types of stiffeners in a disc structure were analysed. Attracted by the potential higher stiffness in the axial direction of a rotor conical structure if compared to a disc structure, the authors recommended a profound study.

The main novelty of this study corresponds to the development of a procedure for the design of cost-effective and dynamically efficient rotor structures employing a rotor conical structure as a case study. A 3MW offshore wind turbine generator rotor conical structure has been statically and dynamically optimised making use of a parametric approach. The structure was optimised from a static point of view, considering that it is working under the worst-case scenario, and from a dynamic perspective, following a parametric approach coupled with the use of topology optimisation tool. Clarifying results about its capacity to comply with the structural requirements while minimising its dynamic response were obtained from the analyses. The implication of using materials with higher Young's modulus to density ratios in the machine dynamic behaviour is discussed.

This paper consists of four main sections: first is an introductory section that presents the latest advances in the field of generator structural design for renewable energy purposes. In the second section, the steps given in the structural optimisation process are described. The third section is the results section, where the data retrieved from static and modal analyses are introduced. The last section addresses the main findings and suggestions for future investigation paths are given.

## 2. Forces and moments acting on electrical generators

Direct-drive wind turbines are low rotating speed machines with no gearbox in its drivetrain. By eliminating the gearbox, a significant improvement in turbine drivetrain failure rate is seen due to the elimination of rotating parts. However, this means that all the loads are transmitted directly from the wind turbine rotor through the main shaft into the electrical generator structure. Large direct-drive generators are more demanding structurally speaking than conventional generators due to their large surface areas. Generators become very big as to maintain the turbine power rate and knowing that the power of a generator is equal to the product of the machine's torque ' $T$ ' and the angular velocity ' $\Omega$ ', ( $P = T\Omega$ ), very large torques must be developed by direct-drive machines. As the torque developed for an electrical generator can be calculated as

$$T = 2\pi\sigma R^2 l \quad (1)$$

where  $R$  corresponds to the radius of the machine's airgap,  $\sigma$  is the shear stress and  $l$  is the machine axial length, a very large device of considerable mass should be considered. To keep the generator air-gap clearance between the stator and rotor is vital from the design point of view. The integrity of the entire machine relies on the capacity of the supporting structure to maintain the airgap open and stable. Different loads are acting on a radial-flux electrical generator such shear, normal, gravitational and thermal, as well as centrifugal forces and wind turbine loading.

The shear stress/torque transmission is generated in the area near the airgap where mechanical energy is transformed into electrical energy. In the steady state, the shear force on the rotor is met by an equal but opposite shear force on the stator. That shear force on the stator comes about as current in the slots and the associated magnetic field interacts with the rotor magnetic field (See Figure 2(a)).

The normal stress, also named as Maxwell stress, is produced by the effect of attraction that the magnets mounted on the rotor generate between the moving and the stationary parts of the machine. It is the largest load (in the order of 200–400kPa in typical machines) and makes the reduction of machine's weight a difficult task for designers since a stiff and robust structure is needed to withstand it (See Figure 2(b)). A key issue to be considered during assembly, transportation and installation is gravity (See Figure 2(c)). Since large amounts of heat are generated during electrical machines operation, thermal expansion or contraction of generator's parts has to be taken into consideration. Figure 2(d) illustrates how the deformation caused by thermal expansion or contraction of components can produce significant changes in flux density and therefore in the forces acting on the generator structure. Designers need to be also aware of centrifugal forces ( $\sim 3$ kPa). These loads are fairly small at low speeds compared to the others (See Figure 2(e)).

Several investigations have been made on how to produce lightweight structures capable of coping with the significant loads at play within the electrical machine during operation and assembly. However, most of them centred their attention on the first two deflection modes, known as Mode 0 and Mode 1. Deflection can be different at distinct zones of rotor and stator (Tavner and Spooner 2006). Air-gap collapse can take place due to:

- Mode 0: Radial expansion of the rotor or radial compression of the stator.
- Mode 1: Rotor eccentricity (localised deflection).
- Mode 2: Distortion of either or both of the circular surfaces into ellipses.
- Mode  $n$ : Distortion with ripples around the circumferences.

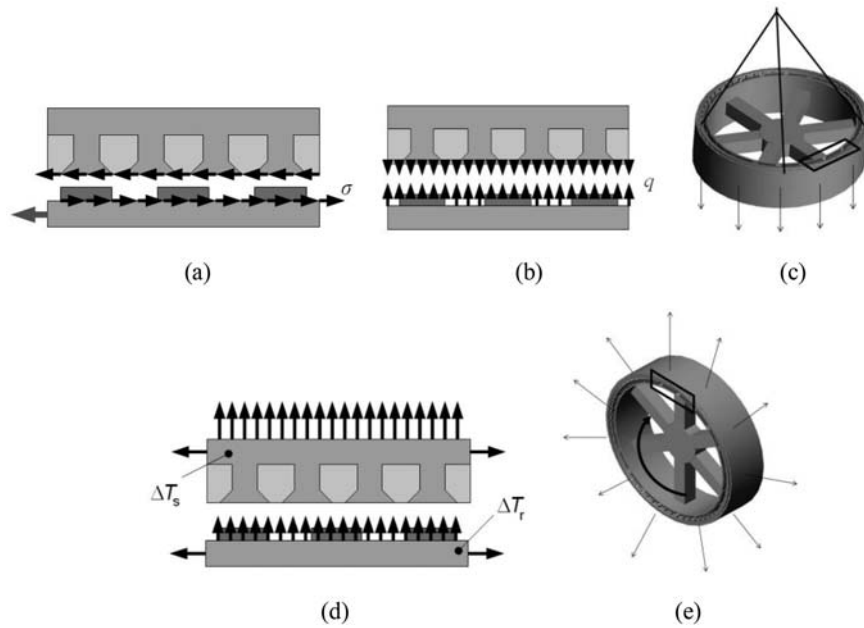


**Figure 2.** (a) Shear loading; (b) Magnetic attraction of the moving and the stationary components of the generator; (c) Gravitational loading; (d) Thermal expansion of the generator structure; (e) Centrifugal loading (McDonald et al. 2008).

Generally, the total variation in airgap clearance can be described as follows,

$$\delta(\theta) = \sum_0^n \delta_n \sin(n(\theta - \varphi_n)) \quad (2)$$

where  $\delta(\theta)$  is the variation in airgap clearance at angle  $\theta$ ,  $\delta_n$  is the amplitude of component  $n$ ,  $\varphi_n$  is the phase angle of component  $n$ , and  $n$  is the number of peaks. The obtained structural pattern results in different deflection modes,

- $n = 0$  for deformation of Mode 0;
- $n = 1$  for Mode 1;
- $n = 2$  for Mode 2;
- $n \geq 3$  for Mode 3 and higher;

A representation of these mode shapes is given in Figure 3. Often the airgap deformation is dominated by a uniform Mode 0 component with amplitude,  $\bar{\delta}$ , and a higher order component with amplitude  $\delta_\Delta$  and hereafter Equation (2) can be altered as:

$$\delta(\theta) = \bar{\delta} + \delta_\Delta \sin(n(\theta - \varphi)) \quad (3)$$

Figure 4 is a plot of the airgap clearance for a prototype generator for a Northern Power 1.5MW direct-drive wind turbine

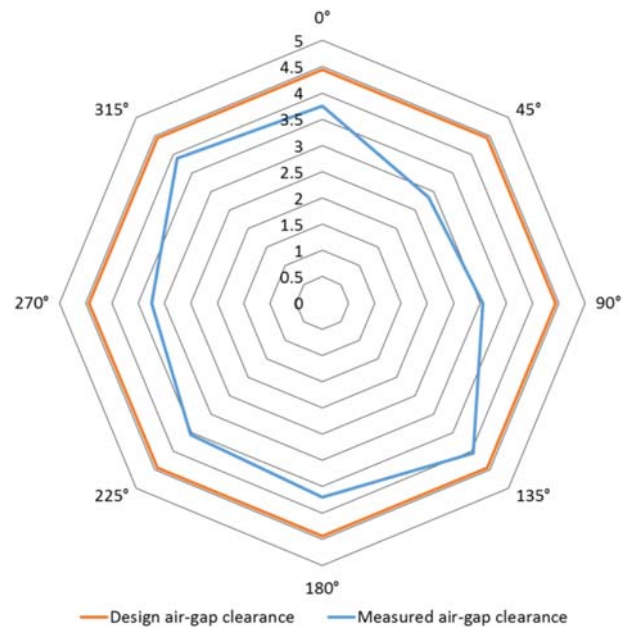


**Figure 4.** Airgap clearance (in mm) for the Northern Power 1.5MW prototype. The values shown here are the mean of the airgap clearance at the upwind and downwind ends of the machine. Clearance is plotted for different angles as seen from the upwind end of the machine. (This figure is available in colour online.)

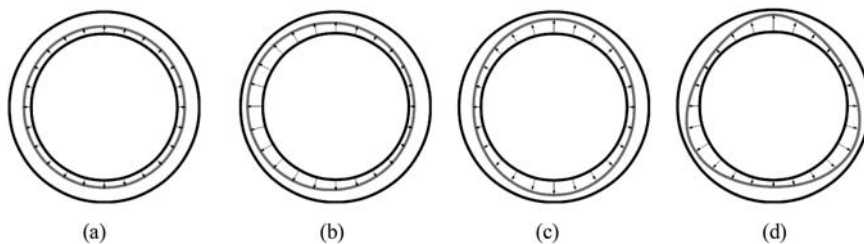


**Figure 3.** A rotor deforming into the airgap towards a stator. (a) Mode 0, uniform deflection,  $\delta(\theta) = \bar{\delta}$ , (b) Mode 1, eccentricity,  $\delta(\theta) = \bar{\delta} + \delta_\Delta \sin(\theta - \varphi)$ , (c) Mode 2, ovalisation,  $\delta(\theta) = \bar{\delta} + \delta_\Delta \sin(2(\theta - \varphi))$ , (d) Mode 3,  $\delta(\theta) = \bar{\delta} + \delta_\Delta \sin(3(\theta - \varphi))$ .

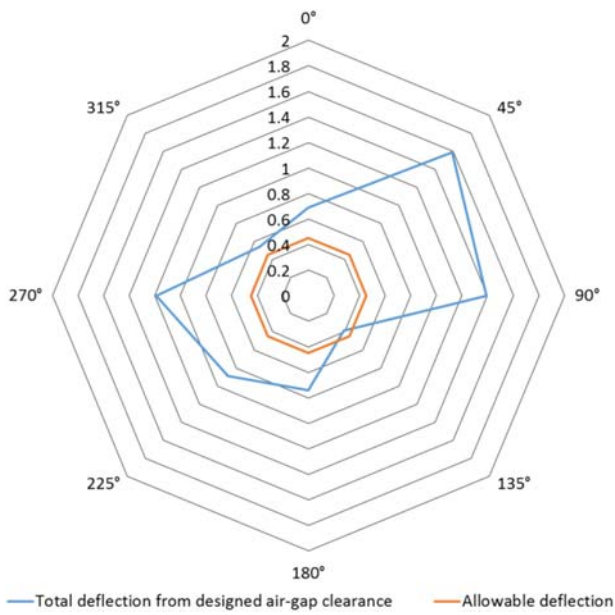


**Figure 5.** Total deflection from designed air-gap clearance (in mm) for the Northern Power 1.5MW prototype. (This figure is available in colour online.)

(Bywaters et al. 2007), showing both the designed and measured airgap clearance, varying with angle. The deflection can be calculated and is shown in Figure 5. The machine shows that the actual deflection exceeds the design limits. In this case the parameters in Equation (3) can be approximated as  $n = 2$ ,  $\bar{\delta} = 9.3\text{mm}$  and  $\delta_{\Delta} = 6.6\text{mm}$ .

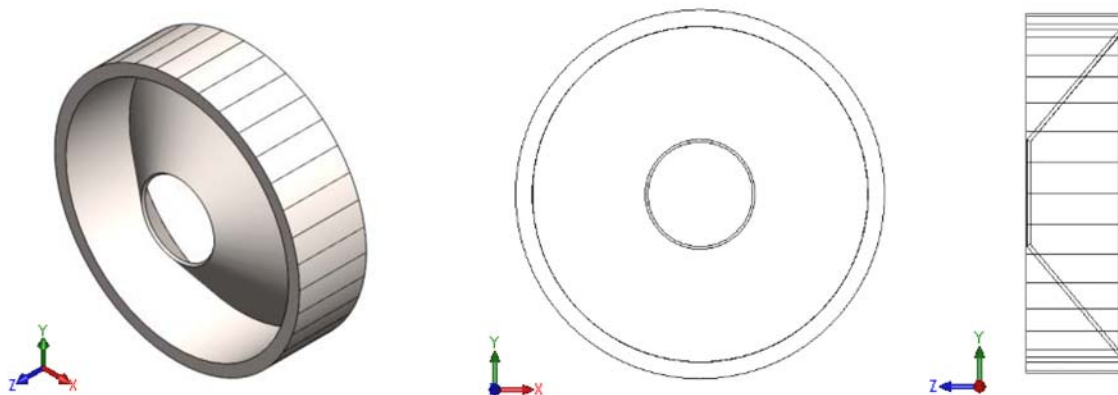
### 3. Methodology

In this section, the proposed methodology for the design of an electrical machine rotor structure is described. In (Jaen-Sola 2017), the author estimated that the difference in mass of structures made with arms and structures made with discs for an electrical machine with the same power rate (3MW) was about 18,500kg. This study was performed for the machine working under typical conditions rather than the worst-case scenario, which indicates that an even heavier and more robust structure would be necessary to cope with the loads. At the same time, the authors proposed the study of rotor conical structures based on the potential extra mass reductions that the introduction in the analysis of other independent variables, such as the cone angle, allows.

This study focuses on electrical generator rotor structures for renewable energy purposes formed by a cylindrical and a conical



(a)



(b)

**Figure 6.** (a) GE rotor conical structure (General Electric 2021); (b) Rotor conical structure 3D CAD model. (This figure is available in colour online.)

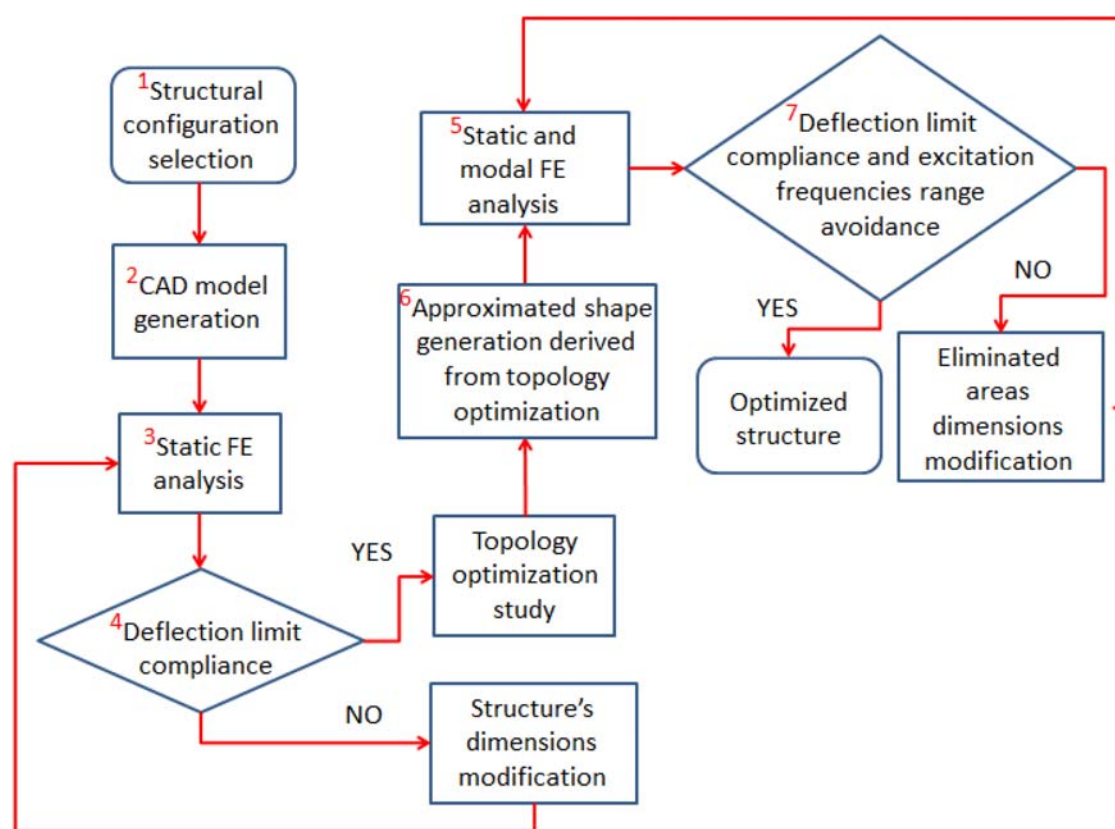


**Figure 7.** Procedure for rotor structural mass optimisation; <sup>1</sup>Step 1: Structural configuration selection; <sup>2</sup>Step 2: CAD model generation; <sup>3</sup>Step 3: Static FE analysis; <sup>4</sup>Step 4: Deflection limit compliance; <sup>5</sup>Step 5: Static and modal FE analysis; <sup>6</sup>Step 6: Approximated shape generation derived from topology optimisation; <sup>7</sup>Step 7: Deflection limit compliance and excitation frequencies range avoidance. (This figure is available in colour online.)

sub-structure. Certain wind energy companies, such as General Electric, 'GE' (General Electric 2021), have typically used this type of structural configurations for electrical machines due to the extra axial stiffness provided by the cone sub-structure that other sub-structures like arms or discs cannot provide, as well as its excellent dynamic characteristics. Figure 6(a) displays a rotor conical structure during the machine assembly operation. In Figure 6(b), the 3D CAD model of the structure is presented.

A variety of rotor structural configurations are available, as shown in Figure 1(a). Once engineers have selected one, an iterative process is followed until the design expectations are met. Stiffeners of triangular shape and ribs are added to the structure in order to increase its stiffness in particular directions and modify its natural frequencies (See Figure 6(a)). In this study, the authors continue the work carried out by Jaen-Sola et al. (2018) to come up with a well-defined methodology that can be tracked when approaching the static and dynamic structural design of the machine. The authors minimised the weight of a 3MW generator rotor conical structure using the ANSYS Design Explorer Optimisation tool. First, a deflection limit equal to 10% of the airgap length in any direction was imposed. Then, the structure's main dimensions, such as cylinder and conical sub-structure thicknesses, were set as independent variables and varied until a combination that met the deflection limit requirement with the lowest weight was found. In this research, the authors use that model and go a step beyond in its optimisation by proposing the use of topology optimisation methods. Bearing in mind that the mass needs to be kept at a minimum to reduce its capital cost and that the energy gathering capability of the machine needs to be maximised, which in turn means that the structural dynamic response needs to be minimised, the authors propose the procedure displayed in Figure 7.

As can be seen in Figure 7, a number of tasks needs to be completed before considering that the structure has been fully optimised. Numbers have been assigned to identify the said tasks that can be described as follows,

1. *Structural configuration selection* – Identification of the turbine to be analysed and its characteristics. By knowing the machine's electrical and mechanical properties one can estimate the loads present during operation and set an appropriate deflection limit and constraint regime. The design characteristics of the turbine studied in this paper are listed in Table 1 for clarification. Then, the rotor structural configuration is selected. As the main goal of this research is to advance the work done by Jaen-Sola et

**Table 1.** Baseline machine design characteristics (Jaen-Sola 2018).

Rated power	3 MW
Rated wind speed	11 m/s
Rated rotational speed	9 rpm
Maximum rotational speed	14 rpm
Cut in wind speed	3.5 m/s
Cut off wind speed	24 m/s
Airgap size	5 mm
Pole pairs	60
Diameter	4 m
Axial length	1.2 m
Aspect ratio	0.3
Structural configuration	Rotor conical
Cone thickness	17 mm
Cylinder thickness	22 mm
Cone angle with horizontal plane	50 degrees
Structural mass	5062kg
Shaft diameter	0.625 m

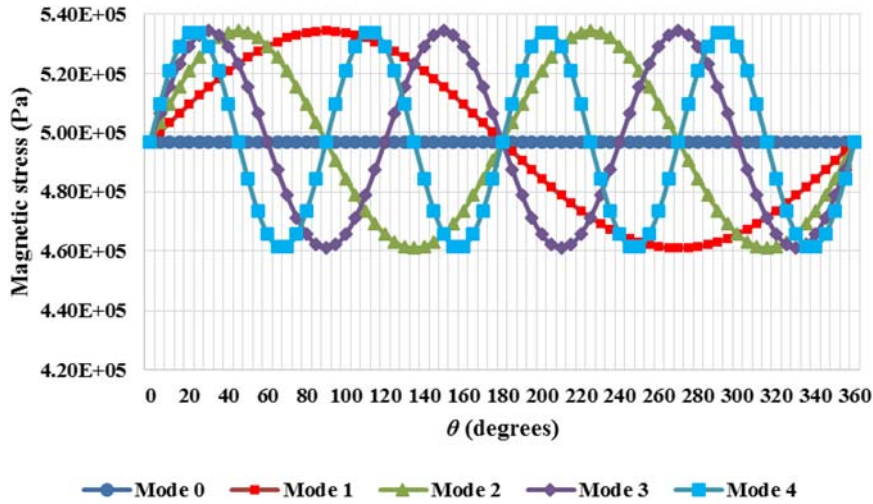


Figure 8. Magnetic stress vs. pitch circumferential angle for different deflection modes (McDonald and Jaen-Sola 2021). (This figure is available in colour online.)

al. (2018), the machine and rotor conical structure presented in this paper has been taken as a benchmark.

2. *CAD model generation* – A 3D CAD model of the structure is generated as one piece following a parametric approach making use of a design table, with a view to reduce the subsequent finite element simulation study setting and run time. With a design table, it is possible to create a set of distinct configurations, for example by modifying one key dimension of the structure while fixing the rest, and simulate them in batch using the same mesh, constraints and loads. It is essential to point out that the parametrisation of the problem through the use of design tables enabling the automation of the process is one of the main novelties of this research.
3. *Static FE Analysis* – At this step the structure is statically analysed. In order to figure out the most critical magnetic attraction deflection mode, the authors made use of the mathematical model derived in (Jaen-Sola 2017; McDonald and Jaen-Sola 2021) for the Maxwell stress calculation. The stresses corresponding to Modes 0, 1, 2, 3 and 4 were computed and applied to the rotor structure in 5 distinct finite element studies. For these studies, the Autodesk Inventor stress analysis package was used. A linear tetrahedral high quality mesh with 29,718 elements and 52,656 nodes obtained from a mesh independence study, with an average element size of 30 mm, was employed. The structure was constrained at the shaft. The Maxwell stress distribution for Modes 1, 2, 3 and 4 can be calculated using

the following expression,

$$\sigma_{PM}(\theta, \bar{\delta}, \delta_{\Delta}) = \frac{\widehat{F}_{PM}^2 \cos^2(p\theta) \mu_0}{2 \left( g + \frac{h_m}{\mu_r} - \bar{\delta} \right)^2} \left[ 1 + \frac{2\delta_{\Delta} \sin(n\theta)}{g + \frac{h_m}{\mu_r} - \bar{\delta}} + \frac{\delta_{\Delta}^2 \sin^2(n\theta)}{\left( g + \frac{h_m}{\mu_r} - \bar{\delta} \right)^2} \right]$$

$$\approx \frac{\widehat{F}_{PM}^2}{4 \left( g + \frac{h_m}{\mu_r} - \bar{\delta} \right)^2} \left[ 1 + \frac{2\delta_{\Delta} \sin(n\theta)}{g + \frac{h_m}{\mu_r} - \bar{\delta}} + \frac{\delta_{\Delta}^2 \sin^2(n\theta)}{\left( g + \frac{h_m}{\mu_r} - \bar{\delta} \right)^2} \right] \quad (4)$$

where  $\sigma_{PM}$  corresponds to the normal component of the Maxwell stress, also known as magnetic stress, for permanent magnet machines,  $\theta$  is the pitch or circumferential angle,  $\bar{\delta}$  is the radial mean deflection and  $\delta_{\Delta}$  is a variable deflection, whose combination gives the total deflection,  $\widehat{F}(\theta)$  is the magnetomotive force set up by the rotor field (winding or magnets) and armature windings current,  $p$  is the number of pole pairs,  $\mu_0$  is the permeability of free space,  $n$ , corresponds to the mode

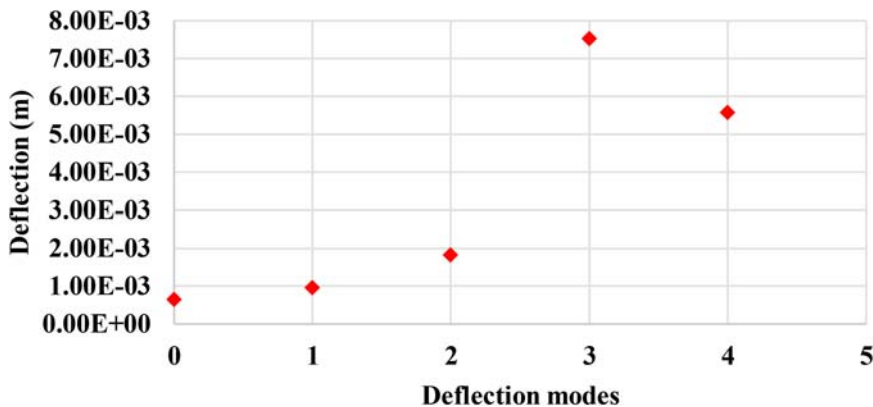
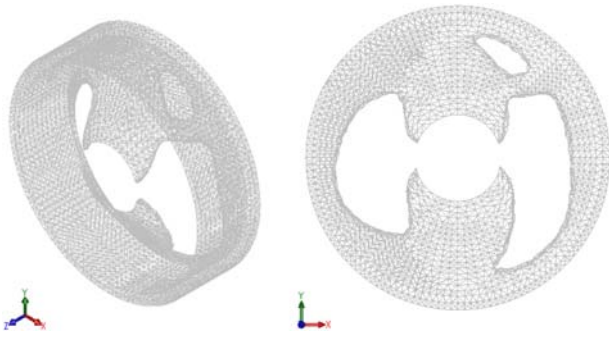


Figure 9. Deflection vs. modes of deflection (cone structure). (This figure is available in colour online.)



**Figure 10.** Topology optimisation of the rotor structure. (This figure is available in colour online.)

of deflection,  $g$  is the nominal airgap clearance,  $h_m$  is the magnet height and  $\mu_r$  is the relative permeability. The equation allows estimating the magnetic stress and its variation with circumferential angle generated by different modes of deflection. A combination of radial mean deflection and a variable deflection obtained from assumed variations in the generator airgap length, like those displayed in Figure 3, are used to calculate the total deflection corresponding to each mode that are then utilised in Equation (4) to calculate the stress.

Since with this equation, the stress can be calculated for an area covering a chosen pitch circumferential angle  $\theta$  and considering that the angle employed in these calculations is equal to 10 degrees, the surface of the cylindrical sub-structure of the rotor was apportioned into 36 different parts so that the appropriate stresses corresponding to Modes 0, 1, 2, 3 and 4 could be applied. Figure 8 shows a plot of the magnetic loads corresponding to the different modes of deflection.

The retrieved results from the five finite element analyses revealed that Mode 3 matched the worst-case scenario with a deflection of  $7.53 \times 10^{-3}$  m, as it can be observed in Figure 9. With the deflection experienced by the structure, it was possible to evaluate the structural stiffness of the generator rotor. Other investigations have looked primarily at Modes 0 and 1. Yet, as observed in Figure 9 these modes are not representative of the real structural behaviour of the machine under extreme loads.

It is important to highlight that as Jaen-Sola et al. (2018) did, it was assumed that the generator was isolated from the turbine hub with the use of an elastic coupling and from the turret by assuming

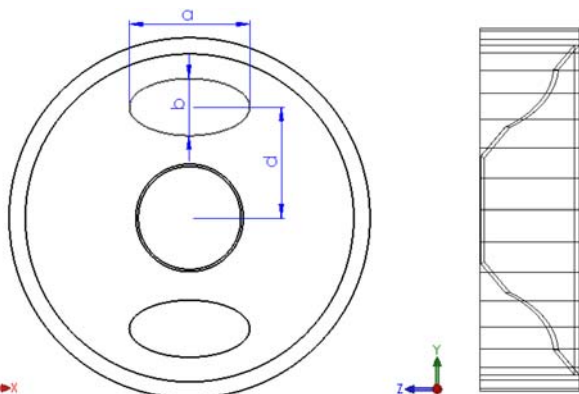


**Figure 11.** Detailed view of the optimised rotor conical structure. (This figure is available in colour online.)

an ideal elastomer-hydraulic damped connection preventing mechanical stresses to be transmitted.

For this study, the authors considered the application of magnetic attraction loading (Mode 3), shear (30kPa) and gravitational ( $9.81 \text{ m/s}^2$ ) loading, as well as thermal (constant temperature of  $55.69^\circ\text{C}$  on the whole structure) and centrifugal (corresponding to 14rpm) loadings. Shear and gravitational loadings are the same as used by Jaen-Sola et al. (2018), whereas the temperature for the thermal loading was taken from the SCADA data presented by ORE Catapult (2020) for a 7MW offshore machine and the centrifugal loading was applied based on the turbine's maximum assumed rotational speed of 14 rpm. This ensured that the authors were able to study the model working under the static worst-case scenario.

4. *Deflection limit compliance* – The process for the mass minimisation of the cast iron (Young's modulus,  $E = 2.1 \times 10^{11} \text{ Pa}$ , Poisson's ratio,  $\nu = 0.3$  and density,  $\rho = 8,000 \text{ kg/m}^3$ ) made sub-structures forming the rotor, cylinder and cone commenced at a first instance by performing a set of FE static simulations where the thickness of one sub-structure was fixed while the one of the other was modified in steps of 5mm using the design table and vice versa. Analyses were carried out considering the deflection limit of 0.5mm until the combination of the thicknesses gave the highest reduction in mass.
5. *Static and Modal FE Analysis* – Once the main dimensions of the structure are adjusted, a topology optimisation study that allows finding the areas not contributing or contributing less to carry the loads was performed. The piece of software utilised in this analysis was the Autodesk Inventor stress analysis package and its embedded Autodesk NASTRAN topology optimisation tool. It did not allow the consideration of neither thermal nor centrifugal loads. However, as the largest loads could be taken into account the analysis was still considered of interest. The same mesh settings were used.
6. *Approximated shape generation derived from topology optimisation* – Data obtained from this study can be used to produce an easy to manufacture the structure capable of withstanding the loads. By approximating the shape and converting its dimensions into independent variables that can be easily modified in a parametric table, engineers can appreciate the structural variations and how they affect the total deflection, the Von Mises stress and their locations in every study in a more visual manner. With this, the problem is simplified and simulations can be run again in batch diminishing the simulation set up time in a substantial manner.
7. *Deflection limit compliance and excitation frequencies range avoidance* – The main dimensions of the approximated shape are changed and static and modal analyses are performed in order to understand the consequences of these dimensional variations in its dynamic behaviour while considering the imposed deflection cap. This new way of characterising the resulting structure will help engineers to develop more integrated and optimal designs capable of taking into account several features at the same time. Fatigue damage and noise can be produced by any mode shape if excited. Due to this, the structural natural frequencies must be eluded or passed as quickly as possible. The excitation frequencies that can activate this structure are (Zavvos 2013),
  - Wind turbine rotational speed frequency (1P), also known as  $\Omega$ .
  - Fundamental electrical frequencies ( $pP$ , with  $p$  being the number of pole pairs)
  - The rotor blades passing in front of the tower frequencies (3P and 6P)



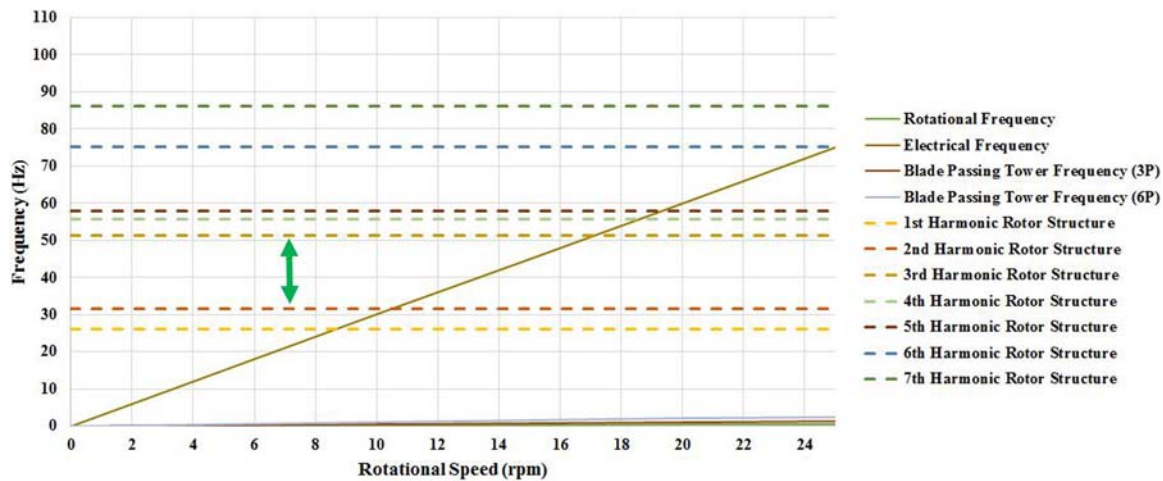


Figure 12. Interference diagram of the system. (This figure is available in colour online.)

As mentioned, one static study, checking that the deflection limit was maintained, was run after each modal analysis. In this research, the first 7 mode shapes in each case were found with no loading applied. Therefore any stiffness or damping effect derived from electromagnetic phenomena was neglected. With the structure fully optimised and since resonant frequencies are directly related to the Young's modulus of the materials, the structural material may be changed so as to understand how its selection affects the wind turbine energy harvesting capability. A comparison between a structure made of cast iron and a structure made of cast alloy steel ( $E = 1.9 \times 10^{11}$  Pa) is presented in Section 4.

#### 4. Results

The baseline structural characteristics used for this study were presented in Table 1. Applying all the loads as listed in step 3 of Section 3, the thickness of both cone and cylinder sub-structures were increased by 5mm in order to find which one added more mass (step 4). It was seen that the cylinder was the sub-structure to concentrate the attention on. Its thickness was increased in steps of 5mm, while the cone thickness was kept constant, until the variation in total deflection was almost negligible. At that moment, cone thickness was increased in the same way until the effect of the growth in cylinder thickness could be noticeable again. This process was repeated 3 times, accounting for 62 simulations in total, until it was seen that the structure was capable of withstanding all the loads without deforming more than 0.5mm in any direction. The final thickness of the cone was 70mm, whereas the final thickness of the cylinder was 198mm. The total mass of the structure was 33,524kg. This represents more than 6.5 times the weight given by Jaen-Sola et al. (2018) for the structure under Mode 0. It is important to highlight that thanks to the thermal loading the stress was well spread across the cone sub-structure.

With the dimensions optimised, the topology optimisation study was performed to obtain the results displayed in Figure 10 (step 5). As observed, it would be possible to make two large cuts as well as to extract a good portion of the inner elements of the right-hand side of the cone sub-structure.

The final shape obtained was not easy to manufacture; hence a more standard profile following the pattern retrieved from the topology analysis was generated (step 6) (See Figure 11). The symmetry of the system was considered as another constraint to maintain the balance of masses. This resulted into two mirrored ellipses that accounted for around 410kg of mass reduction each. The

introduction of a larger number of ellipses was attempted achieving deflection values that went well over the imposed limit. With the optimal number of extruded cuts encountered, the dimensions of both ellipses were modified using again a parametric table. By changing the location of the cuts, ' $d$ ', and the dimensions ( $a$ : major axis;  $b$ : minor axis) it was seen that stiffness and natural frequencies of the whole structure changed in a linear manner.

It is important to point out at this stage that no previous investigations have been performed for generator structures working under these conditions (Mode 3). The mass reduction obtained in this investigation can be considered very modest especially if compared with the expected total value, which accounts for tens of tones. The focus here is to find the best way to produce the lightest structure possible. The 410kg decrease was principally acquired from the elimination of the areas suggested by the software during the compliance based topology optimisation study. The final shape is shown in Figure 11.

The location of the cuts was modified first, followed by the length of the major axis and finally the minor axis. Starting from random values, such as  $d = 1,100$ mm,  $a = 1,088$ mm and  $b = 676$ mm, it could be observed that the deflection decreased with the increase in dimensions, down to a certain limit, which corresponded to  $d = 1,350$ mm,  $a = 1,468$ mm and  $b = 696$ mm. Parameters were varied by fixing two of them and increasing the remaining one in steps of 10mm. The structure's natural frequencies went up in steps of about 0.3Hz with each individual dimensional variation (step 7). The drop in deflection allowed a further reduction of the thickness of one of the sub-structures. As stated in Jaen-Sola et al. (2018), the reduction of cone thickness supposes a fall in the first mode shapes. Then, the cone thickness could be brought down to 58mm and with it the natural frequencies were reduced by almost 4Hz. The mass went down to 30,922kg.

Figure 12 shows an interference diagram of the system, where the natural frequencies of the structure are plotted with the potential excitation frequencies for comparison.

As it can be understood, it is crucial to analyse the consequences of modifying the structure in the dynamic behaviour. From the diagram, it is observed that the rated rotational speed of 9rpm falls directly between the first two mode shapes. The existing gap between the second and the third mode shapes corresponding to the green arrows needs to be enlarged in order to avoid the electrical frequency and maximise the machine operating range, which as it can be seen in the diagram is between 11 and 17rpm. It is not possible to decouple the first two modes from the third one by

altering the main dimensions of the structure or those of the approximated shape as these modes change in the same direction (up or down) almost in the same proportion. Instead, a less dense material ( $7,300\text{kg/m}^3$ ) with a similar Young's modulus ( $E = 1.9 \times 10^{11}\text{Pa}$ ), such as cast alloy steel, was explored. By changing the material of the structure, the deflection value went down again making a further reduction in cone thickness possible, this time to 45 mm and bringing down the natural frequencies by 14%, with the second mode shape reducing from around 32 Hz down to 27.5 Hz and allowing the machine to operate within a range commencing at around 9 rpm (rated rotational speed). The total mass achieved was 28,126 kg, which meant a decrease of almost 10% if compared with the cast iron structure.

## 5. Conclusion

With the main aim of coming up with an efficient methodology for the design of large direct-drive wind turbine electrical generators that minimises the structural mass and the structural dynamic response while complying with the imposed deflection requirements, a parametric approach has been followed. In particular, the conical supporting structure of a 3 MW offshore wind turbine electrical generator rotor has been used as the case study. By using a parametric table and considering the structure's main dimensions and the approximated shape dimensions as independent variables modifications have been gradually made. The effects of these changes have been analysed through a series of finite element static and modal studies. Results showed that the topology optimisation analysis helped to find that by removing certain areas it is possible to increase the overall stiffness of the structure allowing the designer to reduce its volume with the consequent drop in mass and in natural frequencies. This is of interest due to the reduction of the natural frequencies helps to avoid them so the operating range of the machine increases and energy from the wind can be gathered at lower wind speeds. At the same time, the mass drop implies a significant decrease in the turbine capital cost and therefore in the cost of energy as the entire drivetrain would cost less. Moreover, the amount of material required for the turbine tower and foundations would be less and their cost would fall in a substantial manner.

Generator structural design is still in its baby steps and it is becoming more relevant as turbines get bigger and are placed further from shore. Due to the cost and confidentiality status imposed to the design of these machines in the wind energy sector it is not currently possible to validate the results with physical test data. However, the utility and validity of this work can be confirmed by going through the available existing research that has been referenced in this paper.

The results of this investigation show that for a conical structure working under the worst-case scenario almost 6.5 times more mass is required to withstand the loads than for the typical working conditions case. It is necessary to perform a previous static analysis over the proposed structure to identify its most dangerous deflection mode so that the engineer can ensure that the worst-case scenario has been studied. The structural material should be taken into consideration at the early stages of the design. Materials with high Young's modulus to density ratios can help to decrease the mode

shapes of the conical structure. It is not possible to decouple the first two modes from the third mode shape by changing the main dimensions of the structure or those of the approximated shape since these modes vary in the same direction almost in the same proportion. Then, materials with high Young's modulus to density ratios should be used for machines with low rated rotational speeds and vice versa. More research in this area is highly recommended.

With the automation of the design process, it is possible to reduce the manufacturing and labour time as well as the material costs. Large amounts of data are generated from these batch simulations allowed by parametric design tables. It would be interesting to consider their use for training an artificial neural network or another type of suitable machine learning technique permitting a more intelligent design.

## Disclosure statement

No potential conflict of interest was reported by the author(s).

## ORCID

E. Oterkus  <http://orcid.org/0000-0002-4614-7214>

## References

- Bywaters G, Mattila P, Costin D, Stowell J, John V, Hoskins S, Lynch J, Cole T, Cate A, Badger C, Freeman B. 2007. Northern power NW 1500 direct-drive generator. Waitsfield, VT: Northern Power Systems Inc., National Renewable Energy Laboratory, Subcontract Rep. NREL/SR-500-40177.
- Carroll J, McDonald AS, McMillan D. 2016. Failure rate, repair time and unscheduled O&M cost analysis of offshore wind turbines. *Wiley Wind Energy J.* 19(6):1107–1119.
- General Electric. 2021. [Accessed 2021 Mar 9]. Available at <https://ge.com/news>.
- Hartkopf T, Hofmann M, Jöckel S. 1997. Direct-drive generators for megawatt wind turbines. European Wind Energy Conference, Dublin, Ireland.
- IEC 61400 International Standard. 2008. Third edition 2005–2008. [Accessed 2020 May 23] [www.iec.ch](http://www.iec.ch).
- Jaen-Sola P. 2017. Advanced structural modelling and design of wind turbine electrical generators [PhD thesis]. Glasgow: Wind Energy Systems CDT, University of Strathclyde.
- Jaen-Sola P, McDonald AS, Oterkus E. 2018. Dynamic structural design of offshore direct-drive wind turbine electrical generators. *Ocean Eng J.* 161:1–19.
- Jaen-Sola P, McDonald AS, Oterkus E. 2019. Lightweight design of direct-drive wind turbine electrical generators: a comparison between steel and composite material structures. *Ocean Eng J.* 181:330–341.
- Kirschneck M. 2016. Mastering electro-mechanical dynamics of large off-shore direct-drive wind turbine generators [PhD thesis]. Delft: TU Delft.
- McDonald AS, Jaen-Sola P. 2021. A new method for coupling structural and magnetic models for the design and optimization of radial flux PM generators for direct-drive renewable energy applications. *IET Renew Power Gener J.*
- McDonald A, Mueller M, Polinder H. 2008. Structural mass in direct drive permanent magnet electrical generator. *IET Renew Power Gener.* 2(1):3–15.
- ORE Catapult. 2020. [Accessed 2020 May 23]. <https://pod.ore.catapult.org.uk/>.
- Stander JN, Venter G, Kamper MJ. 2012. Review of direct-drive radial flux wind turbine generator mechanical design. *Wiley Wind Energy J.* 15(3):459–472.
- Tavner PJ, Spooner E. 2006. Light structures for large low-speed machines for direct-drive applications. International Conference on Electrical Machines, Chania, Greece.
- Zavvos A. 2013. Structural optimisation of permanent magnet direct drive generators for 5 MW wind turbines [PhD thesis]. Edinburgh: University of Edinburgh.